Bergische Universität Wuppertal

Fachbereich Mathematik und Naturwissenschaften

Lehrstuhl für Angewandte Mathematik
und Numerische Mathematik

Preprint BUW-AMNA 04/11

Roland Pulch

Multidimensional Models for Analysing Frequency Modulated Signals

December 2004

http://www.math.uni-wuppertal.de/org/Num/

Multidimensional Models for Analysing Frequency Modulated Signals

R. Pulch

Bergische Universität Wuppertal, Fachbereich C,
Lehrstuhl für Angewandte Mathematik und Numerische Mathematik,
Gaußstr. 20, D-42119 Wuppertal, Germany.

Abstract
In radio frequency (RF) applications, slowly varying signals often modulate the amplitude and frequency of fast carrier waves. A multivariate signal model yields an efficient representation via decoupling the widely separated time scales. Consequently, the differential algebraic equations (DAEs), which describe a corresponding electric circuit, change into warped multirate partial DAEs. On the other hand, the transient behaviour of the circuit can be approximated by a parameter-dependent DAE model including a multivariate structure, too. The properties of this alternative strategy are investigated. In particular, the two multidimensional approaches are compared with respect to the simulation of RF signals.

1 Introduction

The mathematical model of electric circuits yields systems of differential algebraic equations (DAEs), which specify the corresponding transient behaviour. Electric circuits often feature largely differing time scales. Splitting the DAE into subsystems enables to solve each individual part by an adapted time integration, cf. [1]. However, this approach is not adequate, if nearly all arising signals exhibit a common fast time rate.

In communication electronics, for example, slow input signals alter high frequency oscillations. Consequently, solving the circuit's DAE demands an enormous computational effort, since the fastest rate limits the tolerable size of time steps. Alternatively, amplitude modulated signals can be efficiently represented

by means of a multivariate model, which decouples the time scales. Brachtendorf et al. [2] introduced an according multirate partial differential algebraic equation (MPDAE), where corresponding solutions reproduce signals of the DAE exactly.

If the multidimensional model is extended by a local frequency function, then we can analyse frequency modulated signals, too. Narayan and Roychowdhury [7] prepared a warped MPDAE for this purpose. The determination of appropriate local frequencies is crucial for the efficiency of the model. Hence the theoretical and numerical properties of the warped MPDAE system are more sophisticated in comparison to the MPDAE model for constant time scales.

We design another multivariate model, which yields a parameter-dependent DAE system. This strategy can be interpreted as freezing repeatedly the time in the input of the original DAE. Accordingly, the numerical simulation of this model becomes less costly compared to solving the MPDAE system. However, the outcome of the parameter-dependent DAEs reproduces solutions of the circuit's DAE only approximately. Nevertheless, both models exhibit similar solutions for widely separated time scales.

The intention of the paper is to compare the two multidimensional models with respect to their analytical and numerical qualities. We define the problem concerning the simulation of RF signals in Sect. 2. Next the multivariate signal model and the resulting MPDAE model is outlined. In Sect. 4, we introduce the parameter-dependent DAE system and analyse its properties. Sect. 5 includes the connections between both models with respect to characteristic curves. Subsequently, we observe the use of a solution satisfying the parameter-dependent DAE as starting values for the MPDAE approach. The reconstruction of approximations to the circuit's signals is investigated in Sect. 7. Finally, we present numerical simulations using two versions of a Van der Pol oscillator.

2 Problem Definition

Based on a network approach, the mathematical model of electric circuits typically generates systems of *differential algebraic equations* (*DAEs*), see [3]. We write the DAE system in the form

$$\frac{\mathrm{d}\mathbf{q}(\mathbf{x})}{\mathrm{d}t} = \mathbf{f}(\mathbf{x}(t)) + \mathbf{b}(t), \tag{1}$$

where $\mathbf{x} : \mathbb{R} \to \mathbb{R}^k$ are the unknown time-dependent node voltages and branch currents. The functions $\mathbf{q}, \mathbf{f} : \mathbb{R}^k \to \mathbb{R}^k$ represent a charge and a resistive term, respectively. Furthermore, $\mathbf{b} : \mathbb{R} \to \mathbb{R}^k$ specifies independent input signals. We assume $\mathbf{q}, \mathbf{x} \in C^1$ and $\mathbf{f}, \mathbf{b} \in C^0$ in the following.

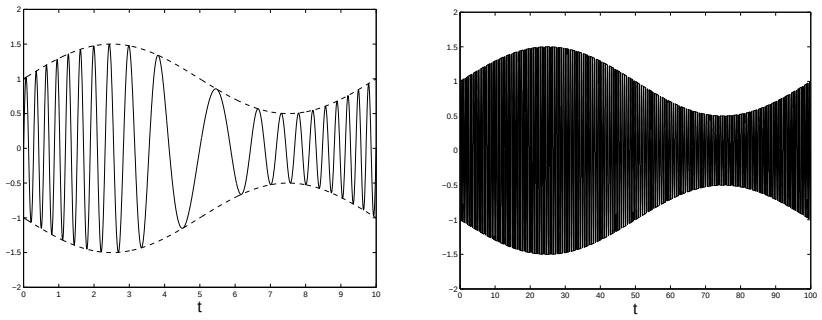

Figure 1: Signal x for time rates $T_1 = 10$, $T_2 = 0.5$ (left) and $T_1 = 100$, $T_2 = 0.5$ (right).

In RF application, we often encounter oscillators. If the input signals are constant, i.e. $\mathbf{b}(t) \equiv \mathbf{b}_0$, then system (1) becomes

$$\frac{\mathrm{d}\mathbf{q}(\mathbf{x})}{\mathrm{d}t} = \mathbf{f}(\mathbf{x}(t)) + \mathbf{b}_0, \tag{2}$$

which is an autonomous DAE now. We assume that this system features a stable periodic steady state response $\mathbf{x}_{\mathrm{per}}$. The corresponding period T_0 is a priori unknown. We may use time or frequency domain methods to determine this solution and its period, see [6]. Since system (2) is autonomous, the shifted function $\mathbf{x}_{\mathrm{per}}(t + c)$ also represents a periodic solution for each $c \in \mathbb{R}$. Accordingly, we require a phase condition to isolate a special solution from this continuum. For example, in time domain, we may apply

$$x_1(0) = \eta \qquad (\eta \in \mathbb{R}), \tag{3}$$

which means that a value of the (without loss of generality) first component of the solution $\mathbf{x} = (x_1, \ldots, x_k)^\top$ is prescribed. The value η must be located in the range of the first component of $\mathbf{x}_{\mathrm{per}}$. Alternatively, a smooth periodic solution exhibits time points, where its derivative vanishes, and those are isolated in general. Hence another possibility is to demand

$$\left.\frac{\mathrm{d}x_1}{\mathrm{d}t}\right|_{t=0} = 0. \tag{4}$$

These phase conditions can be applied as additional boundary conditions in a numerical technique.

Now we consider a time-dependent input signal in (1). Consequently, the inherent time scale T_0 may also vary in time. We assume that the input signal changes at a slow time rate in comparison to fast oscillations of a time scale near T_0. In RF applications, slow input signals change the amplitude and frequency of carrier

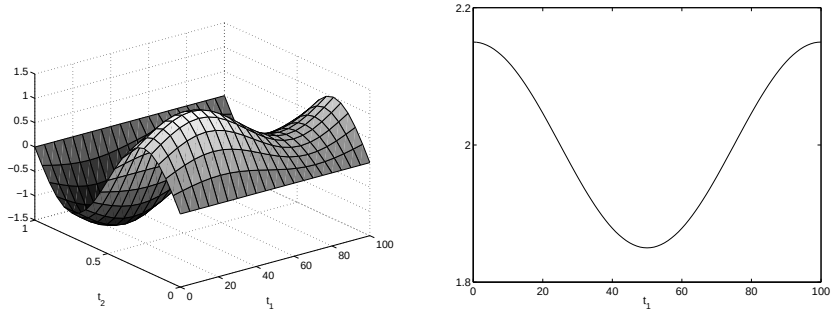

Figure 2: MVF $\hat{x}$ (left) and corresponding local frequency ϑ (right).

waves. The input signals are often periodic, too, which yields the slow rate T_1. A simple instance is the signal

$$x(t) = \left[1 + \alpha \sin\left(\tfrac{2\pi}{T_1} t\right)\right] \sin\left(\tfrac{2\pi}{T_2} t + \beta \sin\left(\tfrac{2\pi}{T_1} t\right)\right) \tag{5}$$

with time rates $T_1 \gg T_2$. Fig. 1 illustrates this signal for $\alpha = 0.5$, $\beta = 15$ and two choices of T_1, T_2. Therefore we require a huge number of time steps to resolve the signal in case of largely differing time scales. Accordingly, transient analysis of the DAE (1) becomes inefficient, since the fast rate restricts the integration step size, whereas the slow rate determines the total time interval of the simulation. Thus alternative techniques for the numerical simulation are needed, which skilfully apply information from the separate time scales.

3 Warped MPDAE Model

A multidimensional model can be used to describe RF signals, which include amplitude as well as frequency modulation. Thereby, we assign an own variable to each disjoint time scale. However, the frequency modulation has to be modelled separately to obtain an efficient representation. In our example (5), we set up the *multivariate function* (*MVF*)

$$\hat{x}(t_1, t_2) = \left[1 + \alpha \sin\left(\tfrac{2\pi}{T_1} t_1\right)\right] \sin\left(2\pi t_2\right), \tag{6}$$

which includes the amplitude modulation part only. This function is biperiodic, where the second period is transformed to 1. Thus the values in the rectangle $[0, T_1[\times [0, 1[$ already fix this function. Fig. 2 shows the MVF, which exhibits a simple behaviour. Hence we sample the MVF using relatively few grid points. The frequency modulation part is described by an additional time-dependent

function

$$\Theta(t) = \frac{t}{T_2} + \frac{\beta}{2\pi} \sin\left(\tfrac{2\pi}{T_1} t\right). \tag{7}$$

We take the derivative $\vartheta := \dot{\Theta}$ as a *local frequency* of the signal (5). In our example, this local frequency results in

$$\vartheta(t) = \frac{1}{T_2} + \frac{\beta}{T_1} \cos\left(\tfrac{2\pi}{T_1} t\right), \tag{8}$$

which is an elementary T_1-periodic function, see Fig. 2. Now we completely reconstruct the original signal via

$$x(t) = \hat{x}(t, \Theta(t)). \tag{9}$$

Thus the second time scale is stretched and we call Θ a *warping function*. Consequently, we obtain an efficient representation of the RF signal by the MVF and corresponding local frequency.

The transition to functions of several variables changes the DAE model (1) into a *warped multirate partial differential algebraic equation* (*MPDAE*)

$$\frac{\partial \mathbf{q}(\hat{\mathbf{x}})}{\partial t_1} + \vartheta(t_1) \frac{\partial \mathbf{q}(\hat{\mathbf{x}})}{\partial t_2} = \mathbf{f}(\hat{\mathbf{x}}(t_1, t_2)) + \mathbf{b}(t_1), \tag{10}$$

where $\hat{\mathbf{x}}$ is the MVF of $\mathbf{x}$. The signals $\mathbf{b}$ operate exclusively at a slow time scale and thus do not require a multidimensional description. We assume that the input signals produce frequency modulation in the solution. Consequently, the local frequency function ϑ depends on the same variable as $\mathbf{b}$.

It follows that a solution of the MPDAE (10) yields a solution of the DAE (1) by the reconstruction (9) with $\Theta(t) = \int_0^t \vartheta(\sigma) \mathrm{d}\sigma$. To solve the MPDAE in a finite domain, appropriate boundary conditions have to be specified using the periodicity. If the input signals are T_1-periodic, then we assume the existence of a biperiodic solution, i.e.

$$\hat{\mathbf{x}}(t_1 + T_1, t_2) = \hat{\mathbf{x}}(t_1, t_2), \quad \hat{\mathbf{x}}(t_1, t_2 + 1) = \hat{\mathbf{x}}(t_1, t_2) \quad \text{for all } \ t_1, t_2 \in \mathbb{R}, \tag{11}$$

together with a T_1-periodic local frequency ϑ. Accordingly, we utilise the rectangle $[0, T_1[\times [0, 1[$ in time domain inclusive biperiodic boundary conditions. A corresponding numerical technique based on the inherent information transport along characteristic curves is investigated in [8].

Given an aperiodic input $\mathbf{b}$, an initial/boundary value problem of the MPDAE system arises, which is sketched in Fig. 3, namely

$$\begin{array}{lrcll} \text{(IC)} & \hat{\mathbf{x}}(0, t_2) & = & \mathbf{h}(t_2) & \text{for all } \ t_2 \in \mathbb{R} \\ \text{(BC)} & \hat{\mathbf{x}}(t_1, t_2 + 1) & = & \hat{\mathbf{x}}(t_1, t_2) & \text{for all } \ t_1 \in \mathbb{R}^+, \ t_2 \in \mathbb{R}. \end{array} \tag{12}$$

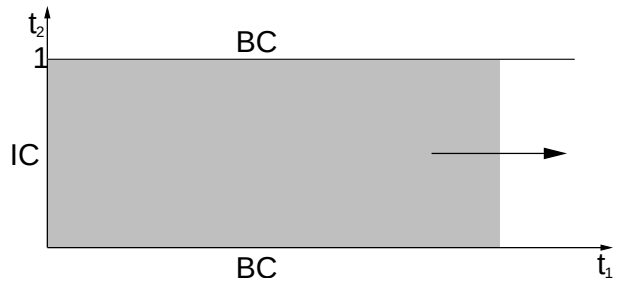

Figure 3: Time domain for initial/boundary value problem of MPDAE.

Thereby, the 1-periodic initial function $\mathbf{h}$ has to be chosen consistent with respect to the DAE (1). Moreover, initial states including identical value $\mathbf{h}(0)$ reproduce the same DAE solution. Thus the choice of initial values influences the efficiency of this approach, too. We may also use problem (12) to determine a biperiodic MVF in case of periodic input. Starting from some initial values, the MPDAE is solved in t_1-direction until the solution reaches a biperiodic steady state response. This technique corresponds to a multidimensional extension of transient analysis.

The MPDAE model demands the determination of an appropriate local frequency function. The local frequency shall provide a simple MVF and thus an efficient multidimensional representation. Hence a suitable local frequency is a priori unidentified. We keep the function ϑ as an additional unknown in the system. Consequently, an extra condition is required to determine the complete solution. Houben [5] proposes a minimum demand, which prevents undesirable oscillations in MVFs. On the other hand, we consider continuous phase conditions, see [7], in the following. These constraints control the phase of the solution in each cross section with constant value t_1. Considering (without loss of generality) the first component of $\hat{\mathbf{x}} = (\hat{x}_1, \ldots, \hat{x}_k)^\top$, we may use

$$\hat{x}_1(t_1, 0) = \eta(t_1) \quad (\eta : \mathbb{R}^+ \to \mathbb{R}) \quad \text{for all } \; t_1 \in \mathbb{R}^+, \tag{13}$$

including a prescribed function η, or

$$\left.\frac{\partial \hat{x}_1}{\partial t_2}\right|_{t_2=0} = 0 \quad \text{for all } \; t_1 \in \mathbb{R}^+. \tag{14}$$

Thus additional boundary conditions arise in time domain. These requirements represent multidimensional generalisations of the phase conditions (3) and (4) from the DAE case. The above phase constraints often yield simple MVFs in solving the MPDAE. However, the efficiency of the resulting multidimensional description can not be guaranteed in general. Therefore the continuous phase conditions represent heuristic choices motivated by the behaviour of RF signals.

Furthermore, the system (10) is autonomous in t_2-direction. Hence if $\hat{\mathbf{x}}$ represents a solution, then the shifted function $\hat{\mathbf{x}}(t_1, t_2 + c)$ satisfies the MPDAE for each $c \in \mathbb{R}$, too. In problem (12), the initial values fix a solution uniquely. On the contrary, using biperiodic boundary conditions, we have to isolate single functions from the continuum of shifted solutions. The additional constraints (13) or (14) are able to perform such a fixing.

More details about the MPDAE model for the case of constant time scales can be found in [10].

4 Parameter-dependent DAE Model

Another multidimensional model corresponding to the DAE (1) is obtained by the following idealisation. Since we assume slowly varying input signals, they are nearly constant in relatively large time intervals. Freezing time in the input yields the DAE

$$\frac{\mathrm{d}\mathbf{q}(\mathbf{x})}{\mathrm{d}t} = \mathbf{f}(\mathbf{x}(t)) + \mathbf{b}(\lambda) \tag{15}$$

with parameter $\lambda \in \mathbb{R}^+$. For fixed λ, the DAE shall exhibit a stable periodic steady state response $\mathbf{x}_\lambda$ with frequency $\varphi(\lambda)$. Applying the normalising transformation $t \to \varphi(\lambda)^{-1}t$ of the time axis, the *parameter-dependent DAE*

$$\varphi(\lambda)\frac{\mathrm{d}\mathbf{q}(\mathbf{x})}{\mathrm{d}t} = \mathbf{f}(\mathbf{x}(t)) + \mathbf{b}(\lambda) \tag{16}$$

for $\lambda \in \mathbb{R}^+$ arises. All periodic solutions $\mathbf{x}_\lambda$ of (16) feature the period 1 now. Each DAE of this family is autonomous. Accordingly, we can use the phase condition (3) or (4) in a numerical time domain method to compute the periodic solution $\mathbf{x}_\lambda$ and its original frequency $\varphi(\lambda)$. If this is done for all λ, we obtain a function

$$\tilde{\mathbf{x}} : \mathbb{R}^+ \times \mathbb{R} \to \mathbb{R}^k, \quad (\lambda, t) \mapsto \mathbf{x}_\lambda(t), \tag{17}$$

which is periodic in t with rate 1 and satisfies ($\tilde{\mathbf{x}} = (\tilde{x}_1, \ldots, \tilde{x}_k)^\top$)

$$\tilde{x}_1(\lambda, 0) = \eta(\lambda) \quad (\eta : \mathbb{R}^+ \to \mathbb{R}) \quad \text{for all } \lambda \in \mathbb{R}^+ \tag{18}$$

or

$$\left.\frac{\mathrm{d}\tilde{x}_1}{\mathrm{d}t}\right|_{t=0} = 0 \quad \text{for all } \lambda \in \mathbb{R}^+. \tag{19}$$

In practice, we solve the DAE model (16) using only a finite set of parameters $0 \le \lambda_0 < \lambda_1 < \cdots < \lambda_n$. If the input signals are T_1-periodic, then we determine a $(T_1, 1)$-periodic function $\tilde{\mathbf{x}}$, i.e. $\lambda_j \in [0, T_1[$ holds.

We are able to solve parameter-dependent DAEs of the family (16) for each parameter λ_j separately. Hence this approach allows ideal parallel computation. Furthermore, $\mathbf{b}(\lambda_j) \approx \mathbf{b}(\lambda_l)$ implies that the DAE has to be solved for just one of the two parameters. If $\mathbf{b}$ includes just a single input signal, then the computational effort decreases significantly, since many recurrences appear in general.

We use the model (16) to get an impression of the oscillator's behaviour. Plotting the function $\tilde{\mathbf{x}}$ as a surface provides a clear visualisation. Moreover, the identification $t_1 = \lambda,\ t_2 = t$ enables a comparison to the MPDAE model. However, it is necessary that $\tilde{\mathbf{x}} \in C^1$ holds for this relation. Accordingly, we assume the existence of a smooth solution of the parameter-dependent DAEs, which satisfies one of the boundary conditions (18),(19). This assumption is as strong as the requirement that a solution of the MPDAE exists, which fulfils one of the continuous phase conditions (13),(14).

In a numerical simulation using the parameters $\lambda_0, \ldots, \lambda_n$, we have to compute separate solutions with correct collective phase to achieve a smooth solution. For each λ_j, several isolated solutions satisfying one of the boundary conditions (18),(19) exist in general. A discretisation of the DAEs yields nonlinear systems, which are solved iteratively by Newton methods. The result corresponding to λ_j represents good starting values in the subsequent step of λ_{j+1}. This choice usually leads to a solution with correct phase. However, the arising sequential structure reduces the potential for parallelism.

The parameter-dependent DAE (16) can also be obtained from the MPDAE (10) by dropping the derivative with respect to t_1. Accordingly, the local frequency ν becomes the frequency function φ. In case of widely separated time scales, the MVFs change relatively slowly in t_1-direction in comparison to the t_2-direction. Hence the idealisation by neglecting the slow derivative is reasonable.

A disadvantage of the model (16) results from freezing the time with respect to input signals. Consequently, we are not able to reconstruct an exact solution of the corresponding DAE (1). On the contrary, the MPDAE approach (10) yields exact signals of the DAE (1) via (9) due to its origin.

5 Characteristic System

In this section, we compare the analytical behaviour of the MPDAE model (10) with the parameter-dependent DAE model (16). The MPDAE system exhibits an inherent hyperbolic structure, see [8]. Accordingly, we arrange the *characteristic*

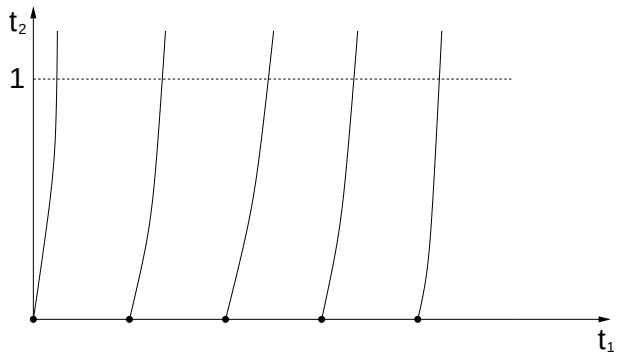

Figure 4: Characteristic projections in domain of dependence.

system

$$\begin{aligned} \tfrac{\mathrm{d}}{\mathrm{d}\tau} t_1(\tau) &= 1 \\ \tfrac{\mathrm{d}}{\mathrm{d}\tau} t_2(\tau) &= \vartheta(t_1(\tau)) \\ \tfrac{\mathrm{d}}{\mathrm{d}\tau} \mathbf{q}(\hat{\mathbf{x}}(\tau)) &= \mathbf{f}(\hat{\mathbf{x}}(\tau)) + \mathbf{b}(t_1(\tau)), \end{aligned} \tag{20}$$

where t_1, t_2 and $\hat{\mathbf{x}}$ depend on a variable τ now. Solutions of the system (20) are called *characteristic curves*. Given a local frequency function ϑ, we solve the first part and obtain

$$\begin{aligned} t_1(\tau) &= \tau + c_1 \\ t_2(\tau) &= \Theta(\tau + c_1) + c_2 \quad \text{with} \quad \Theta(\tau) = \int_0^\tau \vartheta(\sigma)\, \mathrm{d}\sigma \end{aligned} \tag{21}$$

involving integration constants $c_1, c_2 \in \mathbb{R}$. Fig. 4 illustrates some of these *characteristic projections* in case of widely separated time scales. Assuming a high local frequency, it holds $\vartheta(t_1) \geq \vartheta_0 > 0$ for all t_1 and thus the warping function Θ is bijective.

We consider MPDAE solutions, which are periodic in the second coordinate direction with rate 1. Hence we observe the domain $\mathcal{D} := \mathbb{R}^+ \times [0, 1]$, see Fig. 4. Selecting an initial point $(\lambda, 0)$ for arbitrary $\lambda \geq 0$, the characteristic projection

$$\begin{aligned} t_1(\tau) &= \tau + \lambda \\ t_2(\tau) &= \Theta(\tau + \lambda) - \Theta(\lambda) \end{aligned} \tag{22}$$

runs through this point for $\tau = 0$. Only points corresponding to $\tau \in [0, \tau_f]$ are situated in $\mathcal{D}$, where

$$\tau_f(\lambda) = \Theta^{-1}\left(1 + \Theta(\lambda)\right) - \lambda > 0. \tag{23}$$

A transformation of the last part in (20) with respect to a variable $\xi \in [0,1]$ yields the system

$$\frac{1}{\tau_f(\lambda)} \cdot \frac{\mathrm{d}\mathbf{q}(\hat{\mathbf{x}}(\xi))}{\mathrm{d}\xi} = \mathbf{f}(\hat{\mathbf{x}}(\xi)) + \mathbf{b}(\lambda + \tau_f(\lambda)\xi). \tag{24}$$

Now there exist two possibilities how extremely differing time scales arise. Firstly, the local frequency may increase. If $\vartheta(t_1) \gg 1$ holds for all $t_1 \geq 0$, then it follows $\tau_f(\lambda) \ll 1$ for all $\lambda \geq 0$. Consequently, we can approximate the input signal in (24) by $\mathbf{b}(\lambda)$ for all $\xi \in [0,1]$. Secondly, the input signal may become slower, which means that $\mathbf{b}$ is nearly constant even in relatively large time intervals. Therefore the approximation $\mathbf{b}(\lambda)$ for all $\xi \in [0,1]$ is reasonable, too. Hence the system (24) becomes more and more similar to the parameter-dependent DAE (16) in case of increasing differences in time scales. Accordingly, the time intervals τ_f approach the period φ^{-1} in the parameter-dependent DAE. However, we can not perform a transition to the limit case $\tau_f \to 0$, because the system (24) would change completely. This fact indicates that the parameter-dependent DAE is only an approximation for the MPDAE system for fixed time rates.

6 Application as Starting Values

We have seen that the parameter-dependent DAE (16) represents a good approximation for the MPDAE (10) in case of widely separated time scales. Since the computational effort for simulating the parameter-dependent DAE is lower than for the MPDAE approach, the idea is to solve the family of DAEs first and then to use this information for handling the MPDAE.

In the MPDAE system, the local frequency function ϑ is not unique. According choices determine the efficiency of the MVF representation. On the contrary, the function φ in the parameter-dependent DAE is defined as the frequency of periodic solutions. Thus we might think of prescribing $\vartheta := \varphi$ as a good estimate. The MPDAE model can be solved without an additional determination of the local frequency now. Unfortunately, this choice does not work due to a high sensitivity of the problem in case of largely differing time scales. For simplicity, assuming constant frequency $\vartheta \equiv \vartheta_0$, the warping function demonstrates this behaviour. Let T_1 be a slow rate, it follows

$$\Theta(T_1; \vartheta_0 \cdot (1+\varepsilon)) = \int_0^{T_1} \vartheta_0 \cdot (1+\varepsilon)\, \mathrm{d}\sigma = \Theta(T_1; \vartheta_0) + T_1 \vartheta_0 \varepsilon. \tag{25}$$

If $T_1\vartheta_0 \gg 1$ holds, then the relative error ε is amplified significantly. Hence tiny changes of the local frequency result in a large deformation of the corresponding

MVF. Accordingly, we do not expect an a priori specification of local frequencies to yield an efficient representation.

Nevertheless, we use the results of the parameter-dependent DAEs as starting values in Newton methods, which solve nonlinear systems in numerical techniques for the MPDAE. Consequently, the same phase condition has to be used in both models. Since this choice of starting values is near the desired solution, convergence properties of the iteration improve considerably. In comparison to a rough estimate, we require less iteration steps, which leads to a reduction of computation work. However, if the choice is still not sufficient for the convergence of some Newton method, then we apply a homotopy method. The MPDAE system

$$\mu \frac{\partial \mathbf{q}(\hat{\mathbf{x}})}{\partial t_1} + \vartheta(t_1) \frac{\partial \mathbf{q}(\hat{\mathbf{x}})}{\partial t_2} = \mathbf{f}(\hat{\mathbf{x}}(t_1, t_2)) + \mathbf{b}(t_1) \tag{26}$$

includes the homotopy parameter $\mu \in [0, 1]$. For $\mu = 0$, the parameter-dependent DAE arises. The plain MPDAE is obtained for $\mu = 1$. Thus small changes in the homotopy parameter guarantee that the solution of one step represents good starting values in the next step. This technique can also be interpreted in the context of characteristic curves. For small μ, the characteristic projections increase rapidly and reach a line $t_1 = \text{const.}$ in the limit case $\mu \to 0$.

7 Perturbed DAE System

Motivated by (9) in the MPDAE case, we use the solution of the parameter-dependent DAE (16) to reconstruct directly the function

$$\mathbf{y}(t) := \tilde{\mathbf{x}}(t, \Phi(t)) \quad \text{with} \quad \Phi(t) = \int_0^t \varphi(\sigma)\, \mathrm{d}\sigma. \tag{27}$$

Although this signal is not a solution of the original DAE (1), it satisfies a perturbed DAE system. Given a solution $\tilde{\mathbf{x}} \in C^1$ of (16), we calculate the derivative

$$\tilde{\mathbf{s}} := \frac{\partial \mathbf{q}(\tilde{\mathbf{x}})}{\partial \lambda}. \tag{28}$$

Considering the identification $t_1 = \lambda$, $t_2 = t$, the function $\tilde{\mathbf{x}}$ satisfies the modified MPDAE

$$\frac{\partial \mathbf{q}(\tilde{\mathbf{x}})}{\partial t_1} + \varphi(t_1) \frac{\partial \mathbf{q}(\tilde{\mathbf{x}})}{\partial t_2} = \mathbf{f}(\tilde{\mathbf{x}}(t_1, t_2)) + \mathbf{b}(t_1) + \tilde{\mathbf{s}}(t_1, t_2), \tag{29}$$

which is not autonomous in the second time scale any more. Hence the reconstructed signal (27) solves the perturbed DAE

$$\frac{\mathrm{d}\mathbf{q}(\mathbf{y})}{\mathrm{d}t} = \mathbf{f}(\mathbf{y}(t)) + \mathbf{b}(t) + \mathbf{p}(t) \quad \text{with} \quad \mathbf{p}(t) := \tilde{\mathbf{s}}(t, \Phi(t)). \tag{30}$$

In general, the input signals $\mathbf{b}$ occur just in some equations of the system (30). On the contrary, the perturbation $\mathbf{p}$ may influence all components depending on the structure of the function $\mathbf{q}$. In case of widely separated time scales, we expect that the perturbation is small. An a posteriori error estimation can be obtained by the perturbation index concept, see [4]. Let the DAE (1) exhibit perturbation index r and consider a time interval $I := [t_0, t_1]$. If $\mathbf{x}, \mathbf{y}$ are solutions of (1) and (30), respectively, then it holds

$$\begin{aligned} \max_{t\in I} \|\mathbf{x}-\mathbf{y}\| \;\leq\; C \Bigg(& \|\mathbf{x}(t_0)-\mathbf{y}(t_0)\| + \max_{t\in I}\|\mathbf{p}\| \\ & + \max_{t\in I}\left\|\frac{\mathrm{d}\mathbf{p}}{\mathrm{d}t}\right\| + \cdots + \max_{t\in I}\left\|\frac{\mathrm{d}^{r-1}\mathbf{p}}{\mathrm{d}t^{r-1}}\right\| \Bigg), \end{aligned} \tag{31}$$

provided that the terms on the right-hand side are sufficiently small. Thereby, an arbitrary vector norm $\|\cdot\|$ is used. The constant C depends on the DAE (1), its specific solution $\mathbf{x}$ and the interval I but not on the perturbance.

The index 1 case in uncritical, since the right-hand side in (31) can be bounded directly by the maximum norm of $\tilde{\mathbf{s}}$. For index 2, the term $\dot{\mathbf{p}}$ is involved, too, and thus partial derivatives of $\tilde{\mathbf{s}}$ in connection with the function $\dot{\Phi} = \varphi$ arise. However, we can use a numerical solution for $\tilde{\mathbf{x}}$ and φ to calculate a rough estimate of $\|\dot{\mathbf{p}}\|$. In general, a higher index than 2 does not occur in circuit simulation. The ODE case, i.e. index 0, can be included, too, where a bound by the maximum norm of $\tilde{\mathbf{s}}$ is valid like in the situation of index 1.

Hence the relation (31) enables an a posteriori error calculation. Thereby, the quality of the approximation by the perturbed DAE system (30) is estimated. Common applications do not permit an explicit computation of the constant C. Nevertheless, we accept the signal (27) as an adequate approximation for the solution of (1) in case of sufficiently small involved norms of the perturbation. For example, if the perturbation has the magnitude of some physical noise in the underlying electric circuit, then an acceptance of the approximation (27) is obvious. Alternatively, a backward analysis allows for using a numerical solution of the DAE (1) as the exact solution of a perturbed DAE. Consequently, a disturbance $\mathbf{p}$ in (30) with a magnitude of such a perturbation implies that the signal (27) will be an approximation as accurate as the result of a numerical scheme applied to the DAE (1).

8 Illustrative Examples

In our numerical simulations, we consider a Van der Pol oscillator. This benchmark corresponds to an electric circuit, which consists of a capacitance, an in-

ductance and a nonlinear resistor. Adding a voltage source, a forced oscillator arises. We consider the ordinary differential equation (ODE)

$$\begin{aligned} \dot{u} &= v \\ \dot{v} &= -10(u^2-1)v - (2\pi)^2 u + b(t). \end{aligned} \tag{32}$$

Using constant input b, the oscillator produces a periodic response. If a time-dependent input is employed, then the system exhibits frequency modulated solutions. The system (32) represents a stiff ODE. On the contrary, the frequency modulation vanishes in the nonstiff case, cf. [9]. We apply the input signal

$$b(t) = 30 \sin\left(\tfrac{2\pi}{T_1} t\right) \tag{33}$$

with time rates $T_1 = 20,\ 200,\ 2000$. The multidimensional models result in a multirate partial differential equation (MPDE) and a parameter-dependent ODE, respectively. We select the phase conditions (14) and (19). In the MPDE approach, we employ biperiodic boundary conditions. All arising problems are solved by finite difference methods with symmetric differences on uniform grids. The outcome of the parameter-dependent ODE yields the starting values in Newton iterations for solving the MPDE.

Fig. 5 illustrates the local frequencies of the MPDE model and the frequencies of the parameter-dependent ODEs. We observe that the two functions coincide in case of largely differing time scales. Table 1 illustrates the magnitudes of differences between the computed solutions. The more the time scale T_1 becomes slower, the more both multidimensional models agree. Therefore just the MVFs from the MPDE approach are shown in Fig. 6. The shape of MVFs is similar for all three time rates.

Table 1: Maximum differences between solutions from multivariate models.

T_1	$\lvert\vartheta - \varphi\rvert$	$\lvert\hat{u} - \tilde{u}\rvert$	$\lvert\hat{v} - \tilde{v}\rvert$
20	$3.9 \cdot 10^{-2}$	$3.3 \cdot 10^{-1}$	$5.5 \cdot 10^{0}$
200	$3.8 \cdot 10^{-3}$	$3.2 \cdot 10^{-2}$	$5.5 \cdot 10^{-1}$
2000	$3.8 \cdot 10^{-4}$	$3.2 \cdot 10^{-3}$	$5.5 \cdot 10^{-2}$

We use the formulae (9) and (27) to obtain corresponding ODE solutions of (1) and (30), respectively, in the case $T_1 = 2000$. Fig. 7 and Fig. 8 demonstrate the results. For comparison, an initial value problem of (32) was solved via trapezoidal rule. In the first few cycles, all three signals exhibit a good agreement. In later cycles, a phase shift arises, since small numerical errors of the frequency functions amplify during many oscillations.

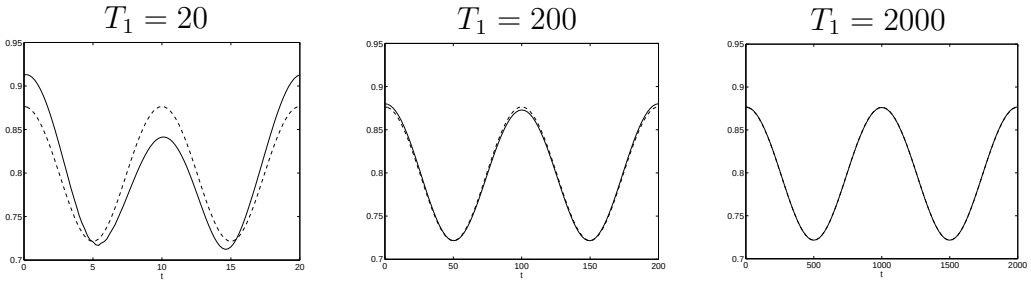

Figure 5: Local frequency of MPDE model (—) and frequency function of parameter-dependent ODE (– –).

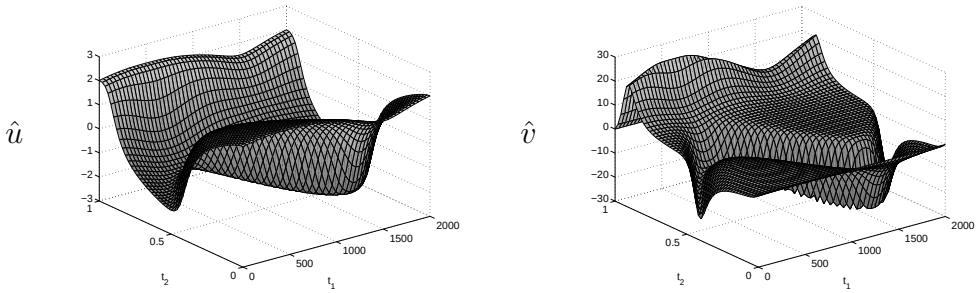

Figure 6: MVFs computed by MPDE model for time rate $T_1 = 2000$.

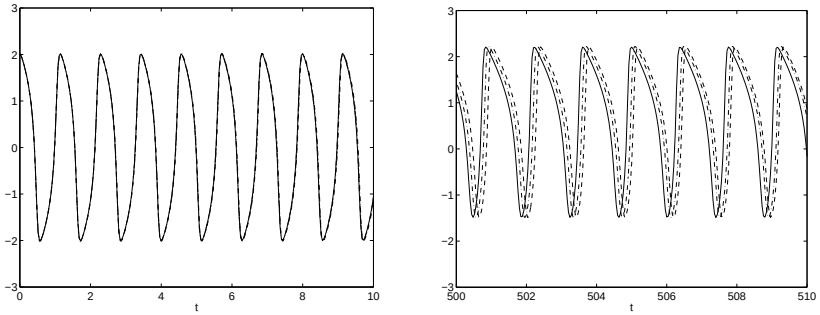

Figure 7: ODE solution u reconstructed by MPDE solution (—) and by parameter-dependent ODE solution (– –) together with integrated reference signal (– · –) in time intervals $[0, 10]$ (left) and $[500, 510]$ (right).

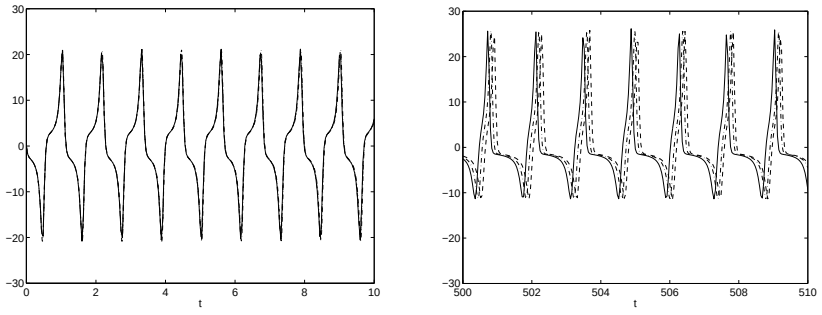

Figure 8: ODE solution v reconstructed by MPDE solution (—) and by parameter-dependent ODE solution (– –) together with integrated reference signal (– · –) in time intervals $[0, 10]$ (left) and $[500, 510]$ (right).

Finally, we also calculate approximately the magnitude of the perturbance (28) corresponding to the reconstructed signal (27). Table 2 illustrates the outcome for the two components. In the three cases, results differ exactly by a scaling with respect to the time rate T_1, since the numerical solutions for the parameter-dependent ODE involve equal values of the input signal. As the derivative in the second equation of the ODE system features a higher magnitude in comparison to the first equation, the same holds for the perturbations, too.

Table 2: Maximum norm of perturbations.

T_1	$\left\lvert\frac{\partial \tilde{u}}{\partial \lambda}\right\rvert$	$\left\lvert\frac{\partial \tilde{v}}{\partial \lambda}\right\rvert$
20	$1.8 \cdot 10^{-1}$	$2.6 \cdot 10^{0}$
200	$1.8 \cdot 10^{-2}$	$2.6 \cdot 10^{-1}$
2000	$1.8 \cdot 10^{-3}$	$2.6 \cdot 10^{-2}$

Furthermore, we investigate a Van der Pol oscillator, where an input signal influences the capacitance term. Thus the corresponding electric circuit represents a voltage controlled oscillator. We formulate the system

$$\begin{aligned} \dot{u} &= v \\ \dot{v} &= -10(u^2 - 1)v - (2\pi w)^2 u \\ 0 &= w - b(t), \end{aligned} \tag{34}$$

which is a DAE of index 1. We consider the input signal

$$b(t) = 1 + \tfrac{1}{2} \sin\left(\tfrac{2\pi}{T_1} t\right) \tag{35}$$

with time rates $T_1 = 20,\ 200,\ 2000$. Again the MPDAE approach and the parameter-dependent DAE model is applied in a numerical simulation, where the settings accord to the previous example.

Fig. 9 depicts the computed local frequency of the MPDAE model, which responds to the input signal. For all three time rates, the frequencies and MVFs of both models exhibit a better agreement than in the previous benchmark. Table 3 demonstrates the quantities. The MVFs computed by the MPDAE approach are shown in Fig. 10. Again the outcome is similar for all periods T_1. The relation between reconstructed univariate solutions behaves like in the previous discussion.

Table 3: Maximum differences between solutions from multivariate models.

T_1	$\lvert\vartheta - \varphi\rvert$	$\lvert\hat{u} - \tilde{u}\rvert$	$\lvert\hat{v} - \tilde{v}\rvert$	$\lvert\hat{w} - \tilde{w}\rvert$
20	$1.3 \cdot 10^{-2}$	$6.0 \cdot 10^{-2}$	$5.6 \cdot 10^{-1}$	0
200	$1.3 \cdot 10^{-3}$	$3.6 \cdot 10^{-3}$	$4.4 \cdot 10^{-2}$	0
2000	$1.3 \cdot 10^{-4}$	$3.6 \cdot 10^{-4}$	$4.4 \cdot 10^{-3}$	0

The magnitude of the arising perturbation (28) corresponding to the parameter-dependent DAE model results to $\left|\frac{\partial \tilde{u}}{\partial \lambda}\right| \leq 3.8 \cdot 10^{-3}$ and $\left|\frac{\partial \tilde{v}}{\partial \lambda}\right| \leq 4.7 \cdot 10^{-2}$ in the case of time scale $T_1 = 2000$. The third component for $\tilde{w}$ exhibits no perturbation, since it represents an algebraic variable of a semi-explicit DAE.

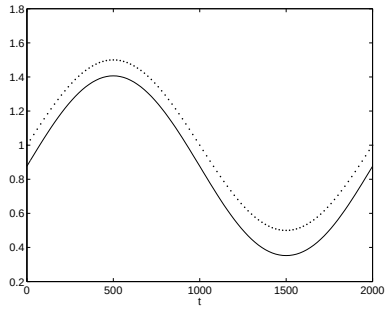

Figure 9: Local frequency of MPDAE model (—) and input signal ($\cdots$) using time rate $T_1 = 2000$.

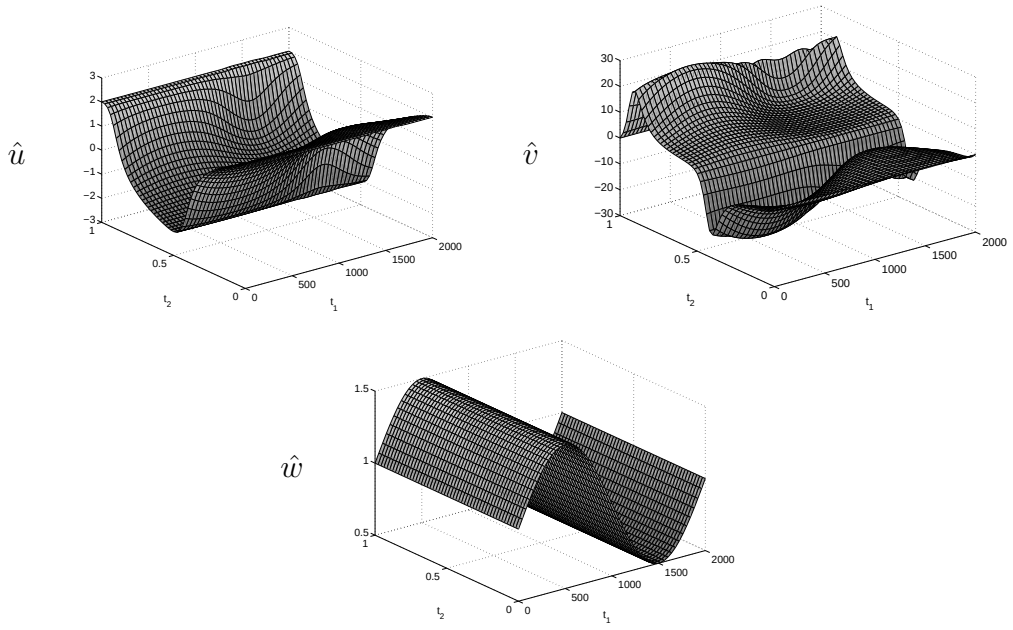

Figure 10: MVFs computed by MPDAE model for time rate $T_1 = 2000$.

9 Conclusions

Two multidimensional models for simulating RF signals have been presented. The MPDAE model reconstructs exact DAE solutions and thus corresponding numerical methods yield the signals for arbitrary demand of accuracy. The parameter-dependent DAE model produces an approximation of the DAE solution, which exhibits a constant error. However, a simulation requires less computational effort and allows more parallelism in the latter approach. Furthermore, the connections between both models permit to use solutions of the parameter-dependent DAEs as starting values for a simulation applying the MPDAE system.

Acknowledgements

This work is part of the BMBF programme "Multiskalensysteme in Mikro- und Optoelektronik" within the project "Partielle Differential-Algebraische Multiskalensysteme für die Numerische Simulation von Hochfrequenz-Schaltungen" (No. 03GUNAVN). The author thanks Prof. Dr. M. Günther (University of Wuppertal) for helpful discussions.

References

[1] Arnold, M.; Günther, M.: Preconditioned dynamic iteration for coupled differential-algebraic systems. BIT 41 (2001) 1, pp. 1-25.

[2] Brachtendorf, H. G.; Welsch, G.; Laur, R.; Bunse-Gerstner, A.: Numerical steady state analysis of electronic circuits driven by multi-tone signals. Electrical Engineering 79 (1996), pp. 103-112.

[3] Günther, M.; Feldmann, U.: CAD based electric circuit modeling in industry I: mathematical structure and index of network equations. Surv. Math. Ind. 8 (1999), pp. 97-129.

[4] Hairer, E.; Lubich, Ch.; Roche, M.: The Numerical Solution of Differential-Algebraic Systems by Runge-Kutta Methods. Springer, Berlin, 1989.

[5] Houben, S.H.M.J.: Simulating multi-tone free-running oscillators with optimal sweep following. in: Schilders, W.H.A., terMaten, E.J.W., Houben, S.H.M.J. (eds.): Scientific Computing in Electrical Engineering, Mathematics in Industry, Springer, 2004, pp. 240-247.

[6] Kundert, K. S.; Sangiovanni-Vincentelli, A.; Sugawara, T.: Techniques for finding the periodic steady-state response of circuits. in: Ozawa, T. (ed.): Analog Methods for Computer-Aided Circuit Analysis and Diagnosis. Marcel Dekker Inc., New York, 1988, pp. 169-203.

[7] Narayan, O.; Roychowdhury, J.: Analyzing oscillators using multitime PDEs. IEEE Trans. CAS I 50 (2003) 7, pp. 894-903.

[8] Pulch, R.: Multi time scale differential equations for simulating frequency modulated signals. Appl. Numer. Math. 53 (2005) 2-4, pp. 421-436.

[9] Pulch, R.: Numerical techniques for solving multirate partial differential algebraic equations. in: Schilders, W.H.A., terMaten, E.J.W., Houben, S.H.M.J. (eds.): Scientific Computing in Electrical Engineering, Mathematics in Industry, Springer, 2004, pp. 337-344.

[10] Roychowdhury, J.: Analysing circuits with widely-separated time scales using numerical PDE methods. IEEE Trans. CAS I 48 (2001) 5, pp. 578-594.